ENVIRONMENTAL RESEARCH
LETTERS

ACCEPTED MANUSCRIPT • OPEN ACCESS

Synoptic conditions conducive for compound wind-flood events in Great Britain in present and future climates

To cite this article before publication: H C Bloomfield *et al* 2024 *Environ. Res. Lett.* in press https://doi.org/10.1088/1748-9326/ad1cb7

Synoptic conditions conducive for compound wind-flood events in Great Britain in present and future climates

H.C.Bloomfield[1,2],[3] **P. Bates**[1,2], **L.C. Shaffrey**[4,5], **J. Hillier**[6], **A, Champion**[7], **D. Cotterill**[1,2,8], **J.O. Pope**[8], **D. Kumar**[4],

[1] School of Geographical sciences, University of Bristol, Bristol, BS8 1SS, UK
[2] Cabot Institute, University of Bristol, University Road, Bristol, BS8 1SS,
[3] School of Engineering, Newcastle University, Newcastle Upon Tyne, NE1 7RU, UK
[4] Department of Meteorology, University of Reading, Whiteknights Road, Reading, RG6 7BE, UK
[5] National Centre for Atmospheric Science, University of Reading, Whiteknights Road, Reading, RG6 7BE, UK
[6] Geography, Loughborough University, Loughborough, LE11 3TT, UK
[7] Aon, The Aon Centre, 122 Leadenhall Street, London, EC3V 4AN, UK
[8] UK Met Office, FitzRoy Road, Exeter, EX1 3PB, UK

E-mail: hannah.bloomfield@ncl.ac.uk

April 2023

Abstract.

Extreme wind is the main driver of loss in North-West Europe, with flooding being the second-highest driver. These hazards are currently modelled independently, and it is unclear what the contribution of their co-occurrence is to loss. They are often associated with extra-tropical cyclones, with studies focusing on co-occurrence of extreme meteorological variables. However, there has not been a systematic assessment of the meteorological drivers of the co-occurring *impacts* of compound wind-flood events. This study quantifies this using an established storm severity index (SSI) and recently developed flood severity index (FSI), applied to the UKCP18 12km regional climate simulations, and a Great Britain (GB) focused hydrological model. The meteorological drivers are assessed using 30 weather types, which are designed to capture a broad spectrum of GB weather.

Daily extreme compound events (exceeding 99th percentile of both SSI and FSI) are generally associated with cyclonic weather patterns, often from the positive phase of the North Atlantic Oscillation (NAO+) and Northwesterly classifications. Extreme compound events happen in a larger variety of weather patterns in a future climate. The location of extreme precipitation events shifts southward towards regions of increased exposure. The risk of extreme compound events increases almost four-fold in the UKCP18 simulations (from 14 events in the historical period, to 55 events in the future period). It is also more likely for there to be multi-day compound events. At seasonal timescales years tend to be either flood-prone or wind-damage-prone. In a future climate there is a larger proportion of years experiencing extreme seasonal SSI and FSI totals. This could lead to increases in reinsurance losses if not factored into current modelling.

Keywords: extreme wind, flood, storm severity index, compound event, climate change
Submitted to: *Environ. Res. Lett.*

1. Introduction

Extreme winds and inland flooding are the two largest causes of loss to North-West Europe [1]. The individual hazards have been well studied from a loss perspective. However, there is increasing evidence that these hazards can spatially or temporally co-occur over daily [2, 3, 4] to seasonal [5, 6, 7, 8] timescales. A recent paper by Bloomfield et al., [9] confirmed this co-occurrence across all these timescales over the whole of Europe. The relationship between co-occurring meteorological, hydrological and impact-driven wind-flood variables are all different, particularly at short timescales. Daily correlations between GB-aggregate maximum 10m wind gusts and total precipitation are ≈ 0.7, whereas daily correlations between GB-aggregate maximum 10m wind gusts and total river flow are ≈ 0.4. The relationships between flood and wind metrics are smaller for more impact focused variables. Understanding these links between hazards, and their possible implications for catastrophe modelling is critical for accurate representations of loss to clients portfolios. Insights can also be gained for infrastructure operators, maintenance crews and government agencies who need to provide warnings on extreme weather events [10].

A key driver of compound wind-flood events at 1—3 day timescales is the presence of extra-tropical cyclones. Previous studies have shown case studies of compound wind-flood events during named storms [11, 12, 13, 14, 15, 16] or have used cyclone tracking algorithms to show that a storm is present during these compound events [2, 4]. If considering just the flood hazard, De Luca et al., [6] used Great Britain (GB) catchment-level river flow to investigate multi-basin flooding events, finding these are associated with persistent cyclonic and westerly atmospheric circulations (defined using Lamb weather types) and atmospheric rivers. Hillier et al., [7] used a large ensemble of climate model data to demonstrate that individual storms impacting north-west GB either tend to be very wet or very windy, not extreme in both. Although co-occurrence is still more likely than pure random chance. At longer-timescales out to two weeks, a multi-storm hazard could be related to clusters of wind storms [5, 17]. Donat et al., [18] show that over central Europe, stormy days are often associated with westerly weather types and positive phases of the North Atlantic Oscillation (NAO+). [19] also show for Northern Europe the majority of historic winter floods occur during NAO+, and the NAO has a significant impact on flood losses. Although, it is still possible to get extreme storms during other synoptic patterns [18].

Analysis at seasonal timescales showed multi-basin flooding can be correlated with the occurrence of very extreme winds [6], which also extended to potential infrastructure damage from compound wind–flood events [20]. The link between seasonal storminess and the NAO over GB, and most of central-Northern Europe was demonstrated in [21]. The increased number of storms in NAO+ is explained by the larger area of the North Atlantic with suitable cyclone growth conditions [22].

There is a growing interest among the insurance community in understanding how co-occurring risks may be impacted by climate change, although at present very little research is published on this topic due to a lack of available high resolution future climate projections, and flood simulations. Bloomfield et al., [9] highlighted the return period of extreme 1-day wind-flood events may reduce four-fold in a future climate. However, the synoptic conditions associated with these events are still not well understood. Using the same underlying climate models (UK Climate Projections 2018, UKCP18) Pope et al., [23] show an increase in cyclonic and westerly wind conditions, suggesting a shift towards warmer, wetter winters. Across the CMIP6 ensemble there is a general trend of wetter winters [24] with an increasing number of extreme cyclones (and stronger associated extreme winds) towards the end of the century [25]. The UKCP18 ensemble also sees an increase in extreme cyclones by 2100, particularly in the convection permitting simulations [26].

Pope et al., [23] highlight weather patterns likely to be related to winter flooding and see a projected increase in the frequency of these conditions by the end of the century. The winter-mean precipitation during each of these patterns also increases in a future climate [27]. Bates et al., [28] showed climate change results in significant future UK flood risks when the UKCP18 simulations are used as inputs to a catastrophe model.

Despite the growing body of research on individual hazards, the impact of climate change on the synoptic conditions associated with compound-wind flood events still remains unclear. A key challenge associated with modelling the relationship between wind and flood damage is the need for high resolution meteorological data products [29] and hydrological data that can be matched to meteorological indices [9]. The recently develop UKCP18 dataset is therefore an excellent resource to understand the behavior of future wind and flood risks which require high resolution information at as close to asset-level as possible. This study will use the UKCP18 regional climate model simulations to:

- Quantify the large-scale drivers of 1-day compound wind-flood extremes over GB in a present climate
- Understand potential impacts of climate change on the occurrence and severity of these events.
- Understand the seasonal occurrence of compound wind-flood extremes and how this may change in a future climate.

2. Data and Methods

In the following subsections the meteorological data (section 2.1) proxies for wind and flood risk (section 2.2) and meteorological indices to classify extreme events (section 2.3) are presented. All metrics used in this study are calculated during extended winter (October-March) and nationally aggregated.

2.1. Climate Data

The UK Climate Projections 2018 (UKCP18) regional model simulations are used in this study. UKCP18 provides hourly 12km data from 1980–2080 using the Representative Concentration Pathway (RCP) 8.5 climate change scenario, with a 12 member perturbed parameter ensemble [30]. Many previous compound wind-flood studies are focused on the historical period (due to lack of appropriately high resolution data in the future period). The UKCP18 simulations allow us to address this issue.

Hourly instantaneous wind gusts and daily total precipitation are taken from all ensemble members for two periods, 1981-2000 and 2061-2080. Although having high resolution climate data is important for accurately modeling compound wind flood risk, other factors are also important to address. As discussed in [9], daily total precipitation is not an appropriate metric to capture winter fluvial flood risk, due to the lagged response of large catchments to extreme rainfall. Therefore, daily-mean GB-aggregated river flows from the Grid-to-Grid (G2G) hydrological model [31] driven by UKCP18 data, are used to create the flood severity index. Further details of the UKCP-derived river flows are given in [32].

Recent results from [27, 26, 33] show there are potential issues with the ability of the 12km UKCP18 simulations to capture extreme precipitation and wind gusts respectively, when compared to the UKCP18 2.2km convection permitting simulations. However, for this study a key requirement was the availability of corresponding hydrological model simulations created in [31], which were not available for the 2.2km model. [33] show that the 12km and 2.2km simulations are largely similar except over orography, which is not the focus of this study (as there are rarely large exposure centres here). However, exploring these results in the 2.2km convection permitting UKCP18 simulations would be an excellent topic for future work.

2.2. Compound event indices

It is important that as well as appropriate meteorological data, that suitable metrics are used to capture the risks associated with wind and flood risks. If not, the relationships presented may not be accurate [9]. The metrics used to most directly estimate impact in this study are the Storm Severity Index (SSI, in the form used in [34] and [35]) and a new Flood Severity Index (FSI) developed in [9]. These metrics provide an indication of times when a meteorological hazard exceeds pre-defined percentile thresholds (which are chosen based on the potential for losses if they are exceeded). The SSI can be given as:

$$SSI(t) = \sum_{i=1}^{N_i} \sum_{j=1}^{N_j} \left(\frac{v(t)_{i,j}}{v_{i,j}^{98}} - 1\right)^3 \cdot I_{i,j} \cdot L_{i,j} \cdot pop_{i,j}$$

$$I_{i,j} = \begin{cases} 0 & \text{if } v(t)_{i,j} < v_{i,j}^{98} \\ 1 & \text{otherwise} \end{cases}$$

$$L_{i,j} = \begin{cases} 0 & \text{over sea} \\ 1 & \text{over land} \end{cases}$$

Here $v_{i,j}$ is the daily maximum wind gust at longitude i and latitude j. $pop_{i,j}$ is the 2020 population density in a given location, taken from [36]. N_i and N_j show the total number of longitudes and latitudes calculations are performed over respectively. The SSI has been developed based on historical loss and damage data (see [37]). Throughout the paper the SSI and FSI metrics are calculated at daily resolution (t = 1 day) which is the highest temporal resolution common across all climate model inputs. Therefore, $v^{98}_{i,j}$ always represents the gridded daily 98th percentile from October-March.

The Flood Severity Index (FSI) is defined as:

$$FSI(t) = \sum_{i=1}^{N_i} \sum_{j=1}^{N_j} (\frac{q(t)_{i,j}}{q^{99.5}_{i,j}} - 1) \cdot I_{i,j} \cdot L_{i,j} \cdot pop_{i,j}$$

$$I_{i,j} = \begin{cases} 0 & \text{if } q(t)_{i,j} < q^{99.5}_{i,j} \\ 1 & \text{otherwise} \end{cases}$$

$$L_{i,j} = \begin{cases} 0 & \text{over sea} \\ 1 & \text{over land} \end{cases}$$

The form is developed from the SSI with parameters defined in the same way, except here the key hydro-meteorological variable is q, the daily total river flow. The cubic behaviour is removed as this was not required to best represent the relationship between wind and flood losses [9]. The form of SSI used here is well established in the literature and relates well to European Losses [17]. The development and verification of the FSI metric are described in [9]. The metric performs particularly well when verified against the number of UK floods (r=0.74). The FSI does however pick up many small events where no flooding was historically recorded. There is a much better match between the occurrence of extreme events (see [9] for full verification) so the most extreme FSI events are the main focus of this study.

When calculating SSI and FSI for the future UKCP18 period the historical percentiles are used. UKCP18 has been shown to reproduce historical SSI and FSI occurrence and compounding well when compared to the ERA5 reanalysis [38] (see Figure 5 of [9]) and is therefore used in this study with minimal comparison to historical observations. However, equivalent results plots can be found in the supplementary material when relevant.

Three types of compound events are considered in the results. Days in which SSI > 0 and FSI > 0 (which gives an indication of relatively strong winds and river flows somewhere over GB). The other two definitions of compounds illustrate various levels of extreme events: SSI $>$ 95th percentile and FSI $>$ 95th percentile, SSI $>$ 99th percentile and FSI $>$ 99th percentile. These were chosen to be large enough that it is feasible that damage may occur, but not so extreme that we run out of events for rigorous statistics. In this study the focus of the compound events analysis is on daily and seasonal timescales. However, details of periods where multi-day compound events (e.g. consecutive days of SSI and FSI exceeding a relevant threshold) are reported in the Supplementary material for general interest, as these may be particularly challenging to the insurance community.

Throughout the study more FSI events are reported than SSI events, due to the higher spatial resolution of the Grid-to-Grid model data than UKCP18 (and therefore more days when one of the grid boxes exceeds a given threshold). Previous work found that when comparing ERA5 (30km) and UKCP18 (12km) the correlations between wind and flood metrics were consistent, across all resolutions, so we don't believe this to be problematic for the study results.

2.3. Weather Patterns

Daily synoptic conditions are defined using the UK Met Office DECIDER tool, using the methods outlined in [39] and the pattern identifications from [23]. The method assigns each day into a set of 30 weather patterns, which have their own climatological characteristics. These patterns are commonly used for medium-long range ensemble forecasting for multiple applications [39, 40].

The original patterns were created using a non-hierarchical k-means clustering algorithm [41] applied to gridded daily MSLP observations [42] for a North Atlantic-European domain (30° W–20° E; 35°N –70° N) at 5° horizontal resolution for the period 1850–2003. The patterns have since been calculated for the ERA5 reanalysis [43] and UKCP18 global model [23]. For each UKCP18 ensemble member, daily MSLP anomalies are calculated (compared to the mean of the corresponding day of the year for the anomaly period). The MSLP anomalies are then regridded to 5° latitude–longitude resolution over the weather pattern domain. Weather patterns are assigned based on their closest distance (defined as the area-weighted sum of squares difference) at each grid point [39].

There is good agreement between the UKCP18 ensemble representation and of patterns when compared to ERA5 (see Figures 2 and 3 of [23]), where any large differences seen are likely due to the differing spatial resolution of the datasets affecting their ability to capture extreme MSLP anomalies.

This may appear a very large number of patterns, however this allows for a comprehensive classification of UK weather throughout the year. Lower-numbered patterns tend to occur more often in summer, and higher-numbered patterns tend to occur more often in winter. The higher-numbered weather patterns have some of the larger mean sea level pressure (MSLP) anomalies (both positive and negative) and can represent some severe weather circulation type (occurring around 1% of the time). A brief description of the 30 weather patterns and examples of their MSLP composites can be found in Table 1 of [23].

In [39] a classification of eight patterns is also provided (intended to be more useful for seasonal forecasting) which are an an aggregation of the 30 patterns into more large-scale flow conditions (see Figure A1 for MSLP composites of these patterns and see [39] for detailed discussion). For visual clarity in the results sections these eight patterns are used. with specific pattern numbers and descriptions given in the text when appropriate.

3. Results and Discussion

3.1. Historical events

The first step in quantifying the meteorological drivers of compound wind-flood events is understanding when these events predominantly occur. Figure 1 shows the seasonal occurrence of extreme wind, flood and compound events for different levels of extremeness. The top row of Figure 1 shows statistics for all times when the SSI and FSI indicators are greater than zero. SSI and FSI events are common throughout the extended-winter period with the occurrence of both peaking in January, therefore resulting in the most compound events being present in this month as well. The colours on the bar chart demonstrate the pattern assignment from [39]. Rather than retaining all 30 weather patterns the bar charts show a sub-set of 8 key weather types (see Figure A1 for examples of the patterns). Across the whole season the most commonly occurring pattern category is NAO+. A similar result is also seen when the metrics are calculated for historical observations (see Figure A2). The most common weather patterns for SSI, FSI and compound events have cyclones located over the UK (e.g., patterns 26, 29 and 30 from the full 30 pattern classification). These were all highlighted in [23] as patterns likely to be associated with UK fluvial flooding. However, There is a surprisingly large presence of NAO- events on days with non-zero SSI and FSI values, supporting [18] which showed around 5% of storm days (depending on the specific storm definition) occur during NAO- conditions. The presence of UK High Pressure for the FSI events is also notable.

A positive value of SSI or FSI is not necessarily enough for there to be loss or damage. Figure 1 therefore also shows events that exceed the 95th and 99th percentiles during the 1981-2000 period. The most extreme compound events mainly happen in January and February, and are predominantly associated with cyclonic weather types (see Table A1 for more details of the 14 largest events which form the compound P99 composite). A key point here is we see extreme events in the UK High and subsets of the North-Westerly pattern, both of which were not identified in [23] as likely to be associated with fluvial flooding. This shows that the synoptic situation associated with compound wind-flood events are not necessarily the same as just for flood events. We note that when considering the observed period of 1981-2000 in Figure A2 only 31 compound P95, and one compound P99 events are present. This shows the value of using the larger UKCP18 ensemble. The distribution of weather patterns across the different levels of SSI and FSI severity is similar in the observed period, supporting the results of [23] which shows the UKCP18 ensemble represents similar seasonal occurrences of each of the 30 patterns to ERA5. However, we note a difference in the timing of the extreme

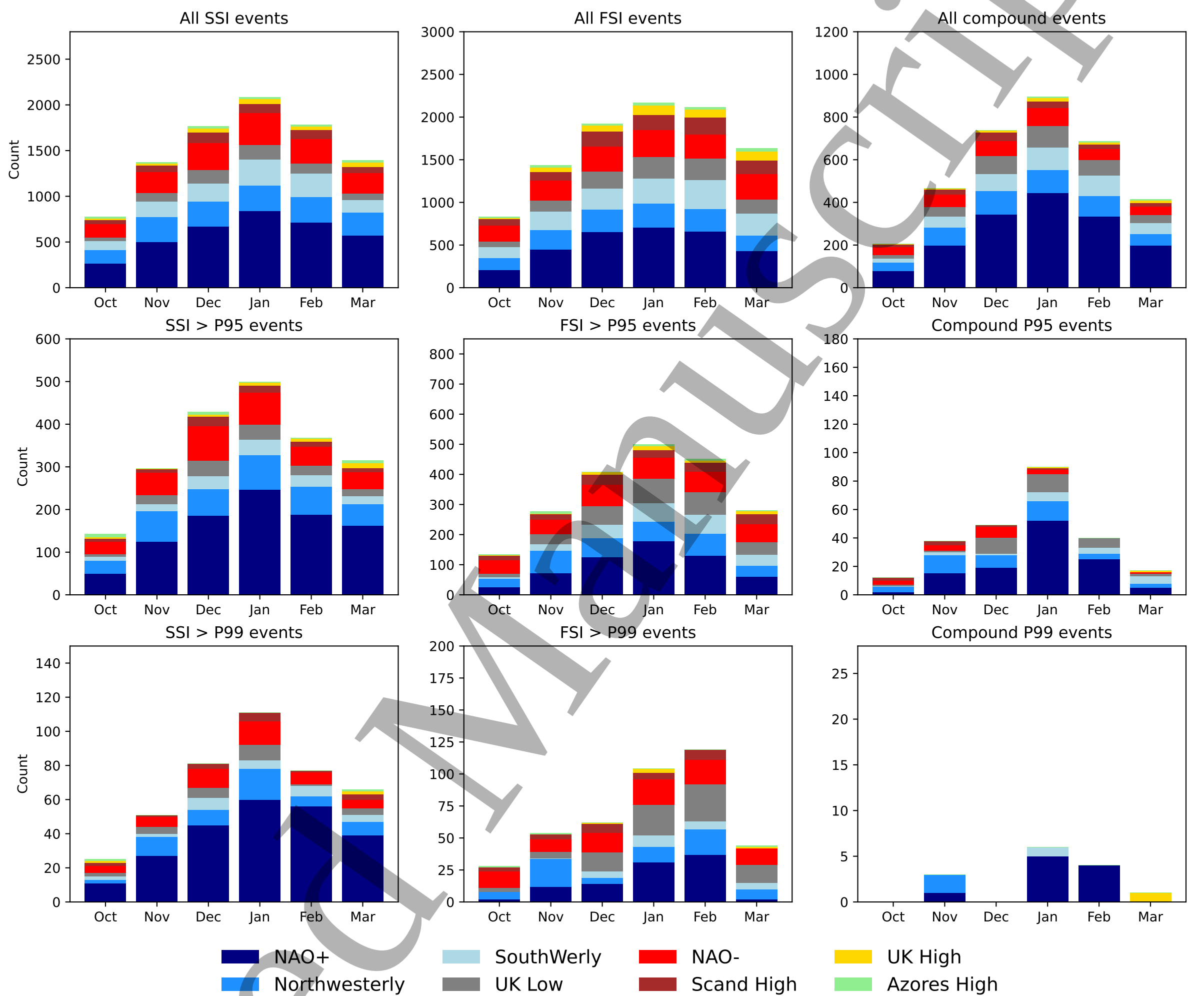

Figure 1. Frequency of SSI (left) FSI (middle) and Compound SSI and FSI events (right) in the historical UKCP18 simulation (1981-2000). Top: All events, Middle: Events exceeding the 95th percentile of the given metrics Bottom: Events exceeding the 99th percentile of the given metrics. Colors indicate the weather pattern on the day of the event, characterized using the met office DECIDER tool (see methods for details). The axis in each subplot are fixed in Figures 1 and 2 for visual clarity.

FSI events in observations (where more occur in early winter). This is likely related to the Grid-to-Grid model setup and an interesting topic to understand in future work.

When examining the most extreme compound events in detail there are two periods where there are multiple consecutive days of extremes (see Table A1). Although there are two multi-day events (consecutive 1-day events), there are no times when two extreme-compound events are seen in the same October-March season. There is also a good spread of events across ensemble members (Table A1).

3.2. Future events

Figure 2 shows the distribution and weather patterns present during the SSI, FSI and compound events in the future (2061-2080) period. We see a 9% reduction in the total number of SSI days, but a 26% increase in FSI days. Overall this leads to a 31% increase in compound events of any magnitude in the future climate, driven by the increase in FSI events. This is consistent with the thermodynamic response to climate change, with the future period of UKCP18 showing a much warmer and wetter climate [44], and therefore increased river flows (see section 3.4 for details). The seasonality of each event type is still similar to the historical period (see Figure 1) and NAO+ is still the most commonly occurring pattern category.

In the future period we see an increase in compound events in February. There is an increase from 14 historical to 55 future compound events exceeding the 99th percentile of SSI and FSI. The details of these are given in Tables A2 and A3. A much smaller proportion of the most extreme events fall outside the December-February period (similar to results from [32] when creating a future flooding event set). In the future period, 20 out of the 55 days are multi-day events (i.e., consecutive 1-day events), suggesting that compound wind-flood events may increase in duration in a future climate. As the events are all $\approx$ 3 days, this is likely due to slower moving individual storms [45] rather than storm clustering. The cyclonic patterns from the NAO+ classification are the most common patterns present during extreme compound events (with 24 and 29 being new additions from the historical period, see Table A1). Increased occurrence of the Northwesterly patterns are seen for the future compound wind-flood events. The presence of a NAO- pattern is particularly interesting as these conditions are not commonly associated with stormy weather over the UK. Section 3.4 will unpick possible reasons for this patterns' presence.

3.3. Synoptic Details

Although the weather pattern analysis in sections 3.1 and 3.2 is useful for broad understanding it is also useful to examine composites of the synoptic conditions during the most extreme events, to understand the details of the assignments. Figure 3 shows daily maximum precipitation composites for the top 14 SSI and FSI events from the historical period and the top 55 events from the future period (see Tables A1, A2 and A3 for details). In both the historical and future periods the most extreme SSI events are associated with strong pressure gradients over southern GB and very high surface wind gusts (see Figure A4) in the region of largest exposure (note that meteorological variables are weighted by population when calculating SSI and FSI). Examining individual events shows storms are present over GB in all cases (see Figure A5 for location of storm centres). These features of the SSI and FSI composites are also seen in the largest events from the observed period (see Figure A3.)

For the FSI events, in both a present and future climate the MSLP gradient is weaker over GB compared to the SSI or compound events. This is due to the variety

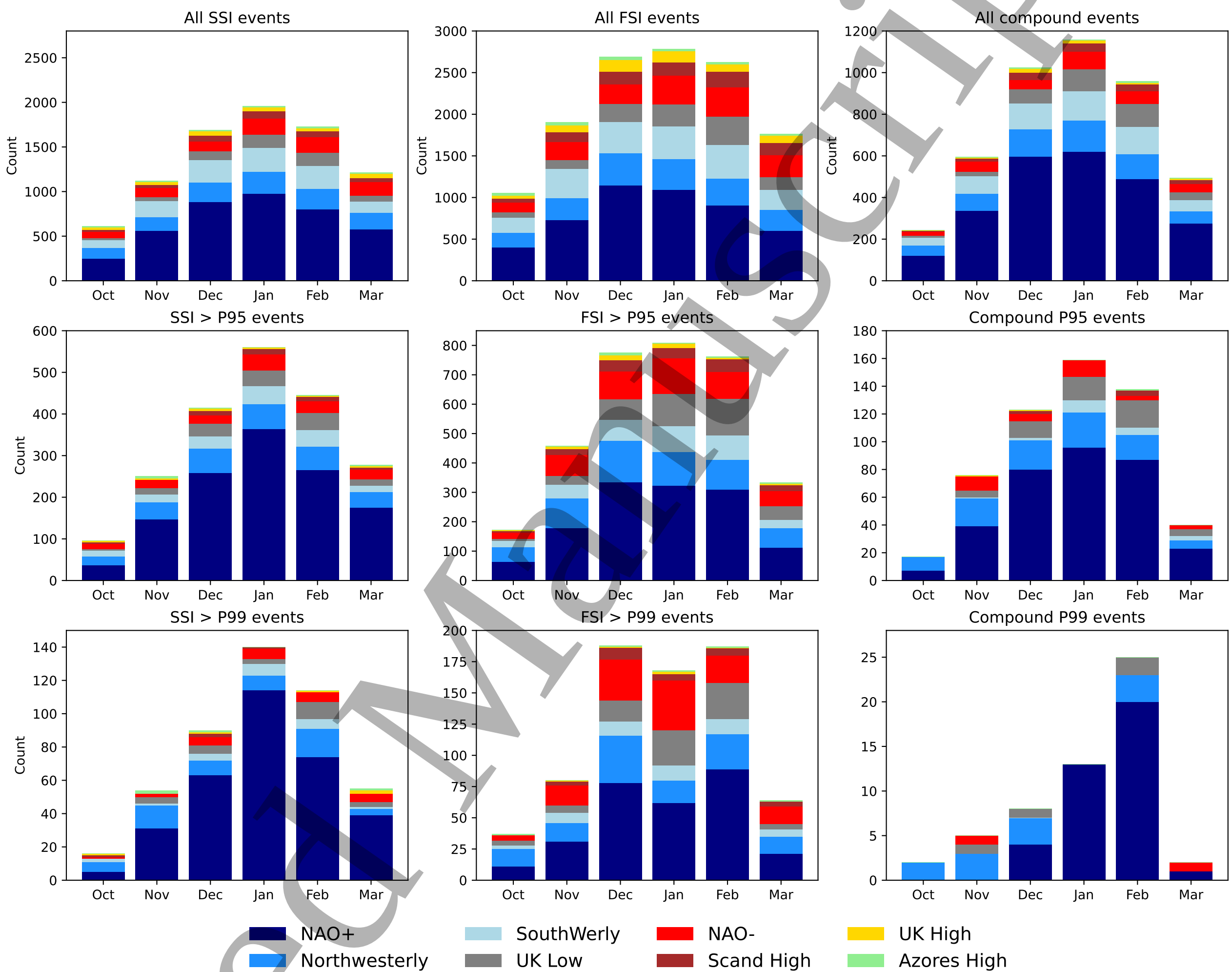

Figure 2. Frequency of SSI (left) FSI (middle) and Compound SSI and FSI events (right) in the future UKCP18 simulation (2061-2080). Top: All events, Middle: Events exceeding the 95th percentile of the given metrics Bottom: Events exceeding the 99ths percentile of the given metrics. Colors indicate the weather pattern on the day of the event, characterized using the met office DECIDER tool (see methods for details). The axis in each subplot are fixed in Figures 1 and 2 for visual clarity.

of large-scale conditions that are leading to extreme GB rainfall (not shown) and the increased number of events in the composite. Despite the larger variation in synoptic conditions there is still a tendency for storms to be located to the North-West of the UK (see Figure A5). The precipitation composites show that extreme FSI events are associated with large rainfall totals over the cities of Northern England, suggesting that many of the compound events may cause damage to different locations across GB rather than spatially co-occurring flood and wind damage (see Figure A4 for potential wind damage).

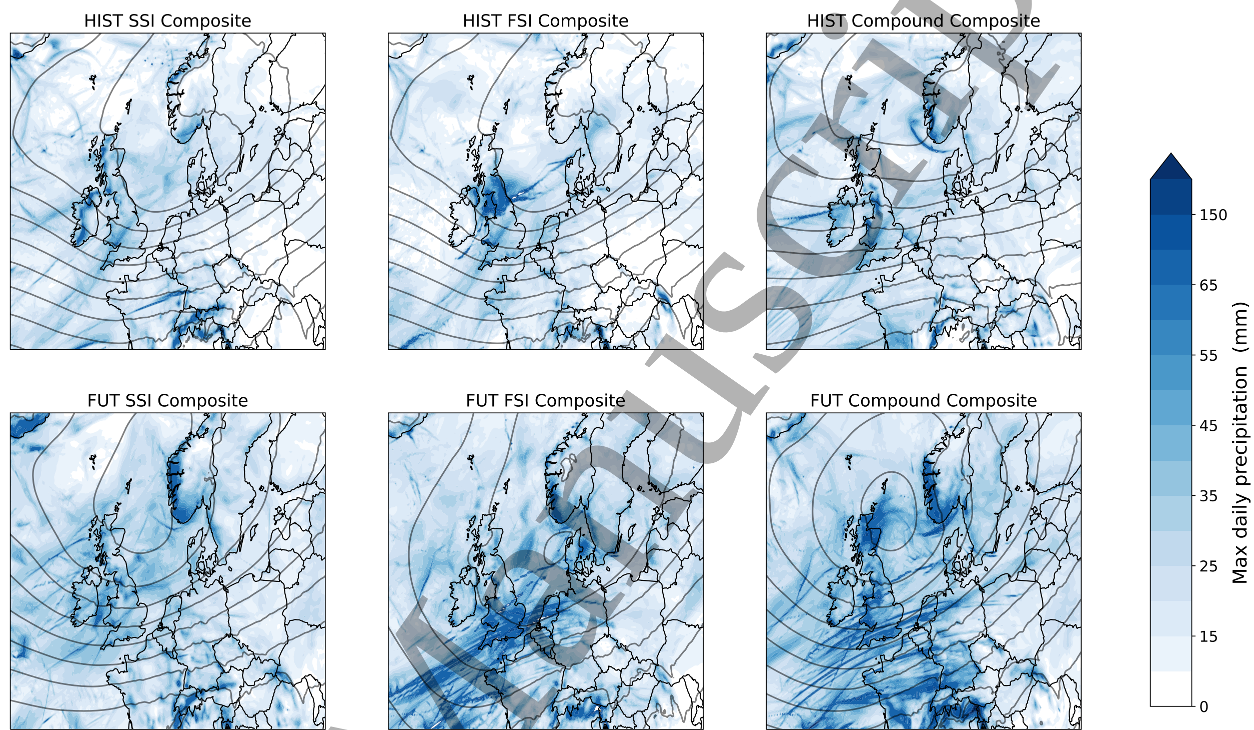

Figure 3. Maximum Daily-total precipitation composites for the largest (99th Percentile) events for SSI (left) FSI (middle) and Compound events (right). Top: Historical UKCP18 period, 1981–2000. Bottom: Future UKCP18 period, 2061–2080. Contours show MSLP composites.

The most striking differences in Figure 3 are the changes in daily maximum precipitation in the future FSI and compound events. The location of most extreme precipitation in the future period is centred over Southern England (as reported in [44]), suggesting extreme rainfall may now coincide with locations of potential wind damage (see Figure A4). This is also a region experiencing increased coastal flood risks, associated with sea level rise [46]. Storms are generally present around GB for the compound wind-flood events, although in a future climate it becomes more common for the minimum MSLP to be over the North Atlantic (see Figure A5). In a future climate the compound event composites look most similar in structure to the future FSI composites. This suggests that in our (much wetter) future climate, the key driver of a compound event is the presence of strong winds on a generally wet day.

3.4. Precursors to compound events

Understanding the weather conditions commonly present during a compound wind-flood event is useful as a first step to develop early warning systems. However, identifying any notable precursor behaviour both seasonally, and just a few days-weeks before and event is also helpful to improve our understanding of the meteorological drivers.

Figure 4 shows the 20-year mean October–March seasonal cycles for key meteorological variables used to generate SSI and FSI. Little change is seen in daily max GB-aggregate wind gusts in the future period, with the timeseries being dominated by climate variability (although we note that extreme wind gusts have been shown to increase in 2.2km spatial resolution UKCP18 simulations, [33]). For precipitation there are notable increases in rainfall from December–February in the future period, which could explain some of the increases in FSI days. The changes in seasonal river flows are more complex, with a notably drier October–November, near-average conditions in December and then a much wetter January–February. The dryer weather in Autumn could be explained by the increases in drier summer-type weather patterns and decreases in stormy weather patterns [44, 47]. This helps to explain why so many of the future FSI events in Figure 2 occur in February. Future work could investigate soil-moisture conditions in the Grid-to-Grid model to identify how saturated catchments are in the lead-up to an extreme FSI event.

Figure 4 shows the GB-aggregate conditions for the three weeks preceding the largest compound events from Tables A1 (solid lines), Tables A2 and A3 (note only the historical events are shown on Figure 4 for clarity). In the historical period GB-aggregate wind gusts are slightly above the climatological average for approximately two weeks before the occurrence of the compound event, with steadily increasing anomalies seen for the 5 days preceding the event. We do however note individual events have quite a range of possible responses (light coloured lines in Figure 4). A similar situation is seen for GB-aggregate river flows and precipitation, but interestingly the largest GB-aggregate precipitation totals are often seen the day *before* the compound event, suggesting a lagged response in the SSI-FSI behaviour, and a potential need for catchments to fully saturate before the most extreme events. This supports analysis from [48] showing that GB-flooding is driven by a combination of extreme precipitation and excess soil moisture (which could be related to high river flows).

3.5. Seasonal occurrences of events

Although the majority of this work is focused on individual days, we also examine the seasonal (October–March) joint behaviour of SSI and FSI as this is useful for setting annual insurance contracts. Figure 5 shows the normalised seasonal occurrence of SSI and FSI (all normalised to the maximum seasonal values from the historical period). Most years in the historical period are either prone to flooding (exceeding 90th percentile of normalised seasonal FSI) or prone to wind damage (exceeding 90th percentile of normalised seasonal SSI) supporting the results of [7]. However, there are

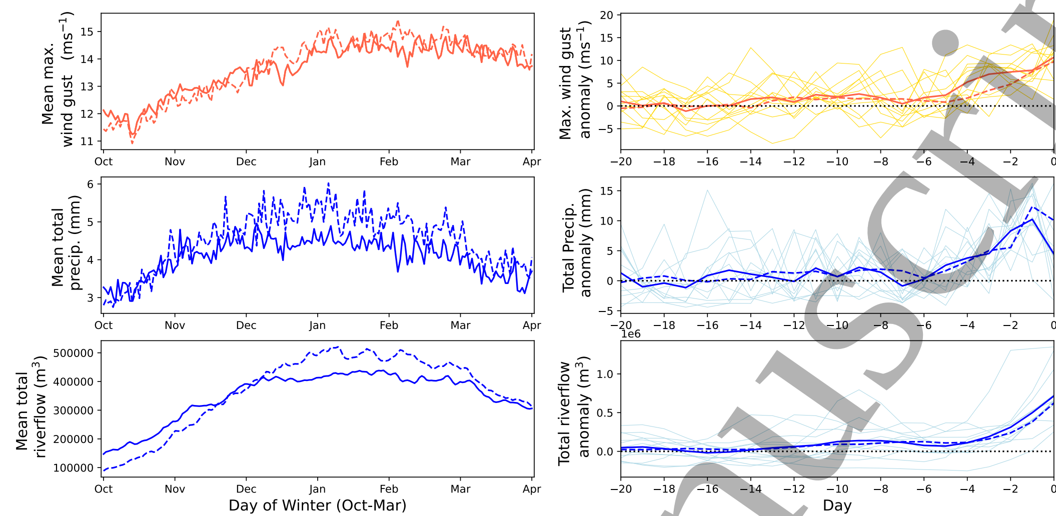

Figure 4. Left: Daily-mean climatology's from October–March for the key variables used to produce FSI and SSI for the historical (solid) and future (dashed) periods. Right: Three weeks of GB-aggregate antecedent weather conditions for the historical extreme compound events (>P99 SSI and FSI, solid lines) and future (dashed lines). Lighter colour lines show the individual events for the historical period.

3 years, marked with red dots which exceed the seasonal 90th percentile of both SSI and FSI (note 2.8 years are expected by random chance, so this is indistinguishable from expectation). In the two largest cases these are single very large multi-day event at the start of February during which the majority of that season's losses occur (see Table A1).

In the future period there are now 9 seasons which exceed the historical 90th percentiles of both SSI and FSI. In these seasons it is now the accumulation of multiple separate wind and flood events leading to the largest seasonal totals, rather than temporally compounding, multi-day events. There are also notably more FSI events than in the historical period.

Figure 5 also shows normalised seasonal SSI and FSI values greater than 1, which means the seasons are more extreme than in the historical period. This is particularly interesting for SSI, as overall we see a 9% reduction in SSI days, here we see it is possible to have much more extreme seasonal SSIs than in the historical period. This may be due to the increased likelihood of sting jets forming in future wind storms [33] which lead to localised intense wind gusts or due to changes in convective storm dynamics [49].

Figure A6 shows the accumulated weather pattern totals for each type of seasonal extreme. Although in a future period a significant number of FSI and compound seasonal totals are seen, when these are normalised by the number of days experiencing an event per season then there are not notable differences between the type of weather patterns seen for each of the SSI, FSI or compound events.

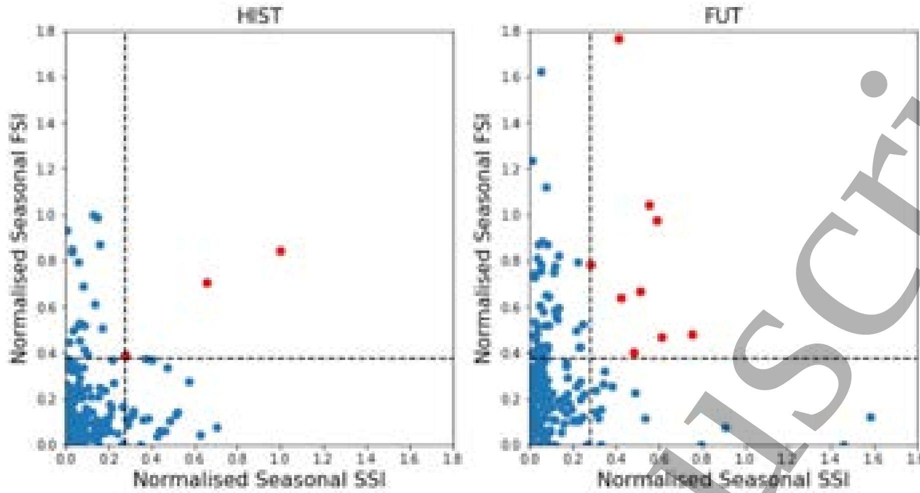

Figure 5. Normalised seasonal totals of SSI vs FSI for the historical period (left, HIST) and future period (right, FUT). Black dashed lines show the historical 90th percentile of SSI and FSI. Red dots show seasons that exceed both of these percentiles.

4. Conclusions

This study has used a set of 30 UK-centred weather pattern classifications defined in [39] to understand the occurrence of, and meteorological drivers of daily and seasonal GB compound wind-flood events in a present and future climate. To define the compound events the SSI index used in [34, 35] and FSI index developed in [9] are used with the previously validated UKCP18 regional 12km dataset. Key results are given below:

- Throughout the study period January and February have the highest risk of daily extreme compound events occurring (exceeding 99th percentile of both SSI and FSI). These events are generally associated with cyclonic weather patterns, often from the NAO+ and Northwesterly pattern classifications (see Figure 1).
- In a future climate, the risk of extreme compound events increases almost four-fold, with 14 events in the historical period, and 55 in the future period. It is also more likely for there to be multi-day compound events (up to 3 days long) in a future climate, and the risk is considerably larger in February than other months. (see Figure 2). However, neither in the current or future climate models runs do we find more than one extreme compound event in a season.
- Extreme compound events happen in a larger range of weather patterns in a future climate, extending the range of patterns identified in [23] for those interesting in potential fluvial flooding (see Tables A1 to A3).
- The most extreme SSI, FSI and compound events are all associated with storms, but the synoptic situation is subtly different for each type of event. In a future climate the region exposed to extreme precipitation shifts from Northern-GB to Southern-GB. Suggesting in future events that these events may be spatially as

well as temporally compounding (see Figure 3).

- In both a present and future climate the most extreme compound events are associated with anomalously high wind gusts and precipitation for around 5 days before the event, but anomalously high river flows for approximately 2 weeks before the event. This could lead to the catchment saturation needed for flooding (see Figure 4).
- At seasonal timescales years tend to be either flood-prone or wind-damage prone. However in a future climate there is a larger proportion of years experiencing both extreme seasonal SSI and FSI totals (see Figure 5).

This study presents insights into the meteorological conditions present during daily compound wind and fluvial flood risk days over GB which extend the recent literature which predominantly uses precipitation as a proxy for flooding [3, 4, 7]. Early warning systems of this type of event are critical to limit the total loss and damage experienced. This type of weather pattern framework is useful when thinking about predictability of compound wind-flood events at medium-range to seasonal prediction timescales [39].

We note that this work uses only one possible future climate scenario. Future work could extend this analysis over a range of future climate models, and climate change scenarios. Different percentiles could also be used for the future SSI and FSI calculations to account for potential future adaptation measures to extreme weather. GB has been used here as a case study due to the interest from the insurance community, but this work could easily be extended to any country where SSI and FSI indices could be calculated and a similar weather pattern classification applied. A final limitation is the treatment of only daily compounds, when we know that floods could occur within several days of a storm first occurring (and therefore well after the time of the extreme winds), particularly in large river catchments. The strongest correlation between wind gusts and river flow over GB have previously been shown to occur at a lag of approximately 2 weeks [9], where persistent synoptic situations could impact local catchment saturation [6, 48]. Understanding the meteorological drivers of compound events over these timescales is also of future interest.

The results also add to the ongoing discussion between meteorological and insurance sectors about the appropriateness of current generation of climate data for modelling and understanding the impacts of extreme meteorological hazards in a present and future climate.

5. Acknowledgements

This work was funded by the Natural Environment Research Council as part of the UK Centre for Greening Finance and Investment (NERC CGFI Grant Number NE/V017756/1). Paul Bates is also supported by a Royal Society Wolfson Research Merit Award. John Hillier is funded by a NERC Knowledge Exchange Fellowship (Grant Number NE/V018698/1). Many thanks are given to the multiple insurance companies who provided feedback on this work and to the AquaCAT project (funded by UK Climate Resilience Programme and lead by Sayers and Partners in association with UKCEH) which developed the future river flow simulations.

6. References

[1] K. Mitchell-Wallace, M. Jones, J. K. Hillier, and M. Foote. *Natural Catastrophe Risk Management and Modelling: A Practitioner's Guide*. Wiley, Oxford, UK, 2017.

[2] T. Matthews, C. Murphy, R. L. Wilby, and S. Harrigan. Stormiest winter on record for Ireland and UK. *Nature Climate Change*, 4:738–740, 2014.

[3] O. Martius, S. Pfahl, and C. Chevalier. A global quantification of compound precipitation and wind extremes: Compound precipitation and wind extremes. *Geophys. Res. Lett.*, 43:7709–7714, 2016.

[4] Laura E Owen, Jennifer L Catto, David B Stephenson, and Nick J Dunstone. Compound precipitation and wind extremes over europe and their relationship to extratropical cyclones. *Weather and Climate Extremes*, 33:100342, 2021.

[5] J. K. Hillier, N. Macdonald, G. C. Leckebusch, and A. Stavrinides. Interactions between apparently primary weather-driven hazards and their cost. *Env. Res. Lett.*, 10:104003, 2015.

[6] P. De Luca, J. K. Hillier, R. L. Wilby, N.W. Quinn, and S. Harrigan. Extreme multi-basin flooding linked with extra-tropical cyclones. *Env. Res. Lett.*, 12(11):114009, 2017.

[7] J. K. Hillier and R. Dixon. Seasonal impact-based mapping of compound hazards. *Env. Res. Lett.*, 15:114013, 2020.

[8] Laura E Owen, Jennifer L Catto, Nick J Dunstone, and David B Stephenson. How well can a seasonal forecast system represent three hourly compound wind and precipitation extremes over europe? *Environmental Research Letters*, 16(7):074019, 2021.

[9] Hannah Bloomfield, John Hillier, Adam Griffin, Alison Kay, Len Shaffrey, Francesca Pianosi, Rachel James, Dhirendra Kumar, Adrian Champion, and Paul Bates. Co-occurring wintertime flooding and extreme wind over europe, from daily to seasonal timescales. *Weather and Climate Extremes*, 39(100550), 2023.

[10] Christopher J White, Daniela IV Domeisen, Nachiketa Acharya, Elijah A Adefisan, Michael L Anderson, Stella Aura, Ahmed A Balogun, Douglas Bertram, Sonia Bluhm, David J Brayshaw, et al. Advances in the application and utility of subseasonal-to-seasonal predictions. *Bulletin of the American Meteorological Society*, 103(6):E1448–E1472, 2022.

[11] A. H. Fink, T. Brucher, V. Ermert, A. Kruger, and J. G. Pinto. The European storm Kyrill in January 2007: Synoptic evolution, meteorological impacts and some considerations with respect to climate change. *Nat. Hazards Earth Syst. Sci.*, 9:405–423, 2009.

[12] M. L. R. Liberato. The 19 January 2013 windstorm over the North Atlantic: Large-scale dynamics and impacts on Iberia. *Weather Clim. Extremes*, 5-6:16–28, 2014.

[13] Raveh-Rubin. Large-scale wind and precipitation extremes in the Mediterranean: A climatological analysis for 1979–2012. *Q. J. R. Meteorol. Soc.*, 141:2404–2417, 2015.

[14] M. Kendon and M. McCarthy. The UK's wet and stormy winter of 2013/2014. *Weather*, 7(2):40–47, 2015.

[15] F. Otto, K. van der Wiel, and G. J. van Oldenborgh. Climate change increases the probability of heavy rains in Northern England/Southern Scotland like those of storm Desmond-a real-time event attribution revisited. *Environmental Research Letters*, 13(2):024006, 2018.

[16] T. Matthews, C. Murphy, G McCarthy, C Broderik, and R. L. Wilby. Super Storm Desmond: a process-based assessment. *Env. Res. Lett.*, 13(1):014024, 2018.

[17] M. D. K. Priestley, H. F. Dacre, L. Shaffrey, K. I. Hodges, and J. G. Pinto. The role of serial European windstorm clustering for extreme seasonal losses as determined from multi-centennial

simulations of high-resolution global climate model data. *Nat. Hazards Earth Syst. Sci.*, 18:2991–3006, 2018.

[18] Markus G Donat, Gregor C Leckebusch, Joaquim G Pinto, and Uwe Ulbrich. Examination of wind storms over central europe with respect to circulation weather types and nao phases. *International Journal of Climatology*, 30(9):1289–1300, 2010.

[19] Stefano Zanardo, Ludovico Nicotina, Arno GJ Hilberts, and Stephen P Jewson. Modulation of economic losses from european floods by the north atlantic oscillation. *Geophysical Research Letters*, 46(5):2563–2572, 2019.

[20] J. K. Hillier, T. Matthews, R. L. Wilby, and C. Murphy. Multi-hazard dependencies can increase and decrease risk. *Nature Climate Change*, 10:595–598, 2020.

[21] Michael A Walz, Markus G Donat, and Gregor C Leckebusch. Large-scale drivers and seasonal predictability of extreme wind speeds over the north atlantic and europe. *Journal of Geophysical Research: Atmospheres*, 123(20):11–518, 2018.

[22] Joaquim G Pinto, Stefan Zacharias, Andreas H Fink, Gregor C Leckebusch, and Uwe Ulbrich. Factors contributing to the development of extreme north atlantic cyclones and their relationship with the nao. *Climate dynamics*, 32:711–737, 2009.

[23] James O Pope, Kate Brown, Fai Fung, Helen M Hanlon, Robert Neal, Erika J Palin, and Anne Reid. Investigation of future climate change over the british isles using weather patterns. *Climate Dynamics*, 58(9-10):2405–2419, 2022.

[24] Intergovernmental Panel on Climate Change (IPCC). *Climate Change 2021 – The Physical Science Basis: Working Group I Contribution to the Sixth Assessment Report of the Intergovernmental Panel on Climate Change*. Cambridge University Press, 2023.

[25] Matthew DK Priestley and Jennifer L Catto. Future changes in the extratropical storm tracks and cyclone intensity, wind speed, and structure. *Weather and Climate Dynamics*, 3(1):337–360, 2022.

[26] Colin Manning, Elizabeth J Kendon, Hayley J Fowler, Nigel M Roberts, Ségolène Berthou, Dan Suri, and Malcolm J Roberts. Extreme windstorms and sting jets in convection-permitting climate simulations over europe. *Climate Dynamics*, 58(9-10):2387–2404, 2022.

[27] Elizabeth J Kendon, Erich M Fischer, and Chris J Short. Variability conceals emerging trend in 100yr projections of uk local hourly rainfall extremes. *Nature Communications*, 14(1):1133, 2023.

[28] Paul D Bates, James Savage, Oliver Wing, Niall Quinn, Christopher Sampson, Jeffrey Neal, and Andrew Smith. A climate-conditioned catastrophe risk model for uk flooding. *Natural Hazards and Earth System Sciences*, 23(2):891–908, 2023.

[29] Jakob Zscheischler, Philippe Naveau, Olivia Martius, Sebastian Engelke, and Christoph C Raible. Evaluating the dependence structure of compound precipitation and wind speed extremes. *Earth system dynamics*, 12(1):1–16, 2021.

[30] Simon O Tucker, Elizabeth J Kendon, Nicolas Bellouin, Erasmo Buonomo, Ben Johnson, and James M Murphy. Evaluation of a new 12 km regional perturbed parameter ensemble over europe. *Climate Dynamics*, 58(3):879–903, 2022.

[31] Alison Kay. Simulation of river flow in britain under climate change: baseline performance and future seasonal changes. *Hydrological Processes*, 35(e14137), 2021.

[32] Adam Griffin, Alison Kay, Paul Sayers, Victoria Bell, Elizabeth Stewart, and Sam Carr. Widespread flooding dynamics changing under climate change: characterising floods using ukcp18. *Hydrology and Earth System Sciences Discussions*, pages 1–18, 2022.

[33] Colin Manning, Elizabeth J Kendon, Hayley J Fowler, and Nigel M Roberts. Projected increase in windstorm severity and contribution from sting jets over the uk and ireland. *Weather and Climate Extremes*, page 100562, 2023.

[34] Joaquim G Pinto, Melanie K Karremann, Kai Born, Paul M Della-Marta, and Matthias Klawa. Loss potentials associated with european windstorms under future climate conditions. *Climate Research*, 54(1):1–20, 2012.

[35] Matthew DK Priestley, Helen F Dacre, Len C Shaffrey, Kevin I Hodges, and Joaquim G Pinto. The role of serial european windstorm clustering for extreme seasonal losses as determined from multi-centennial simulations of high-resolution global climate model data. *Natural Hazards and Earth System Sciences*, 18(11):2991–3006, 2018.

[36] Erin Doxsey-Whitfield, Kytt MacManus, Susana B Adamo, Linda Pistolesi, John Squires, Olena Borkovska, and Sandra R Baptista. Taking advantage of the improved availability of census data: a first look at the gridded population of the world, version 4. *Papers in Applied Geography*, 1(3):226–234, 2015.

[37] M. Klawa and U. Ulbrich. A model for the estimation of storm losses and the identification of severe winter storms in Germany. *Nat. Hazards Earth Syst. Sci.*, 3(6):725–732, 2003.

[38] Hans Hersbach, Bill Bell, Paul Berrisford, Shoji Hirahara, András Horányi, Joaquín Muñoz-Sabater, Julien Nicolas, Carole Peubey, Raluca Radu, Dinand Schepers, et al. The era5 global reanalysis. *Quarterly Journal of the Royal Meteorological Society*, 146(730):1999–2049, 2020.

[39] Robert Neal, David Fereday, Ric Crocker, and Ruth E Comer. A flexible approach to defining weather patterns and their application in weather forecasting over europe. *Meteorological Applications*, 23(3):389–400, 2016.

[40] Robert Neal, Rutger Dankers, Andrew Saulter, Andrew Lane, Jonathan Millard, Gavin Robbins, and David Price. Use of probabilistic medium-to long-range weather-pattern forecasts for identifying periods with an increased likelihood of coastal flooding around the uk. *Meteorological Applications*, 25(4):534–547, 2018.

[41] Andreas Philipp, Paul-M Della-Marta, Jucundus Jacobeit, David R Fereday, Philip D Jones, Andres Moberg, and Heinz Wanner. Long-term variability of daily north atlantic–european pressure patterns since 1850 classified by simulated annealing clustering. *Journal of Climate*, 20(16):4065–4095, 2007.

[42] Tara J Ansell, Phil D Jones, Rob J Allan, David Lister, David E Parker, M Brunet, Anders Moberg, Jucundus Jacobeit, P Brohan, NA Rayner, et al. Daily mean sea level pressure reconstructions for the european–north atlantic region for the period 1850–2003. *Journal of Climate*, 19(12):2717–2742, 2006.

[43] Samuel R Harrison, James O Pope, Robert A Neal, Freya K Garry, Ryosuke Kurashina, and Dan Suri. Identifying weather patterns associated with increased volcanic ash risk within british isles airspace. *Weather and Forecasting*, 37(7):1157–1168, 2022.

[44] Jason A Lowe, Dan Bernie, Philip Bett, Lucy Bricheno, Simon Brown, Daley Calvert, Robin Clark, Karen Eagle, Tamsin Edwards, Giorgia Fosser, et al. Ukcp18 science overview report. *Met Office Hadley Centre: Exeter, UK*, 2018.

[45] Abdullah Kahraman, Elizabeth J Kendon, Steven C Chan, and Hayley J Fowler. Quasi-stationary intense rainstorms spread across europe under climate change. *Geophysical Research Letters*, 48(13):e2020GL092361, 2021.

[46] Rachel J Perks, Dan Bernie, Jason Lowe, and Robert Neal. The influence of future weather pattern changes and projected sea-level rise on coastal flood impacts around the uk. *Climatic Change*, 176(3):25, 2023.

[47] Daniel Cotterill, Peter Stott, Nikolaos Christidis, and Elizabeth Kendon. Increase in the frequency of extreme daily precipitation in the united kingdom in autumn. *Weather and Climate Extremes*, 33:100340, 2021.

[48] W. R. Berghuijs, S. Harrigan, P. Molnar, L. Slater, and J. W. Kirchner. The relative importance of different flood-generating mechanisms across Europe. *Water Resour. Res.*, 55(6):4582–4593, 2019.

[49] Hayley J Fowler, Geert Lenderink, Andreas F Prein, Seth Westra, Richard P Allan, Nikolina Ban, Renaud Barbero, Peter Berg, Stephen Blenkinsop, Hong X Do, et al. Anthropogenic intensification of short-duration rainfall extremes. *Nature Reviews Earth & Environment*, 2(2):107–122, 2021.

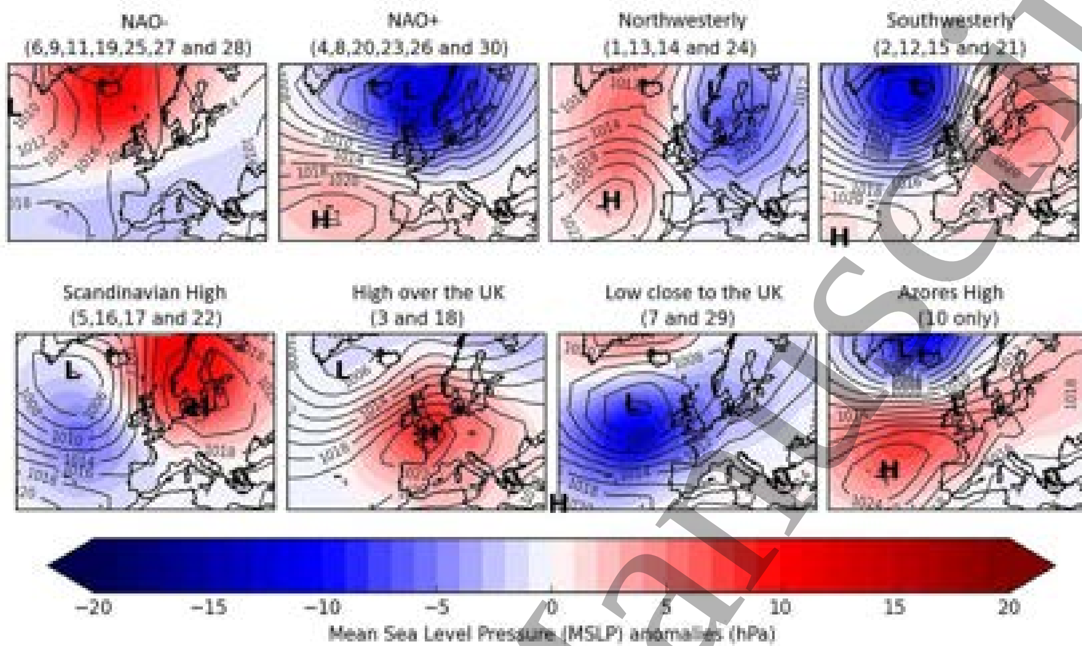

Figure A1. Mean Sea Level Pressure Composites of the 8 weather pattern categories used in this study, adapted from [39]. See Figure 1 of [39] for the full 30-pattern composites.

Appendix A. Supplementary Material

Appendix A.1. Composites of extreme event behaviour

Appendix A.2. Weather Pattern Information

Appendix A.3. Historical compound events

Appendix A.4. Future compound events

Appendix A.5. Additional Composites

Appendix A.6. The impact of climate change on weather pattern occurrence

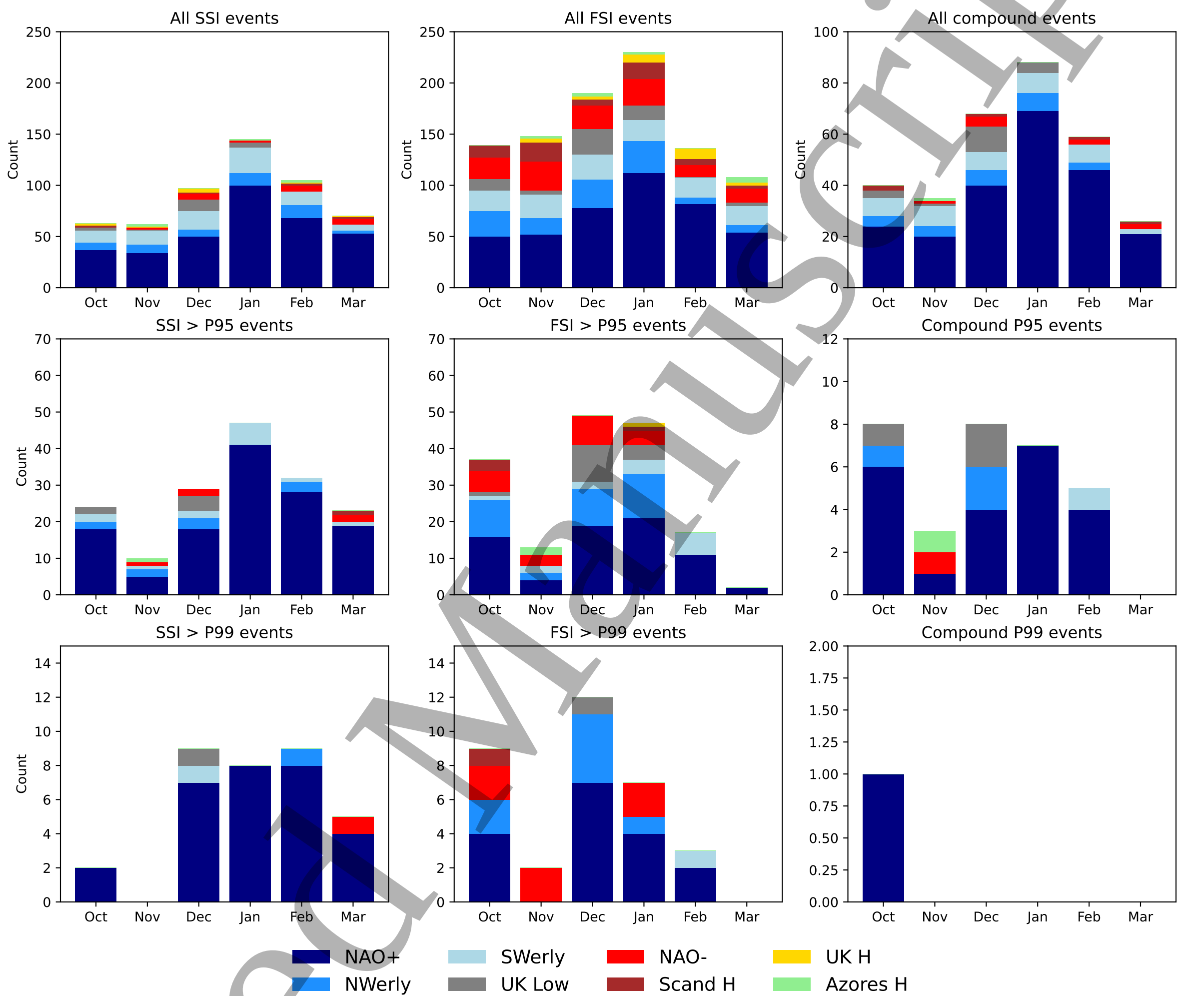

Figure A2. Frequency of ERA5-derived SSI (left) Grid-to-Grid derived FSI (middle) and Compound SSI and FSI events (right) in the historical period (1981-2000). Top: All events, Middle: Events exceeding the 95th percentile of the given metrics Bottom: Events exceeding the 99th percentile of the given metrics. Colours indicate the weather pattern on the day of the event, characterized using the met office DECIDER tool (see methods for details).

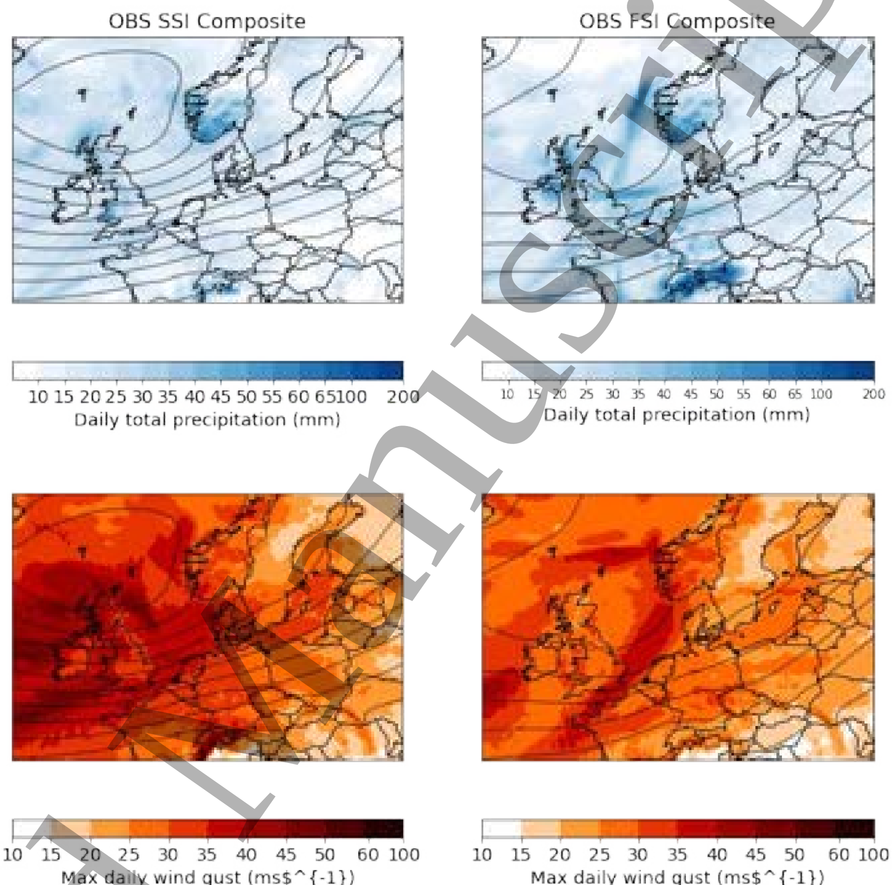

Figure A3. Composites of (top) Maximum Daily-total precipitation (bottom) Daily-maximum wind gusts for the largest (exceeding the 99th Percentile) events for ERA5-derived SSI (left) Grid-to-Grid-derived FSI (right) in the historical period (1981-2000) with data taken from the ERA5 reanalysis. Axis are the same as Figure 3 and Figure A4 for direct comparison with the UKCP18 events. Contours show MSLP composites.

Ensemble Member	Year	Month	Day	Weather Pattern
1	1994	1	4	21
2	1985	11	14	30
2	1994	2	2	30
2	1994	2	3	30
2	1994	2	4	30
3	1991	2	2	30
4	1992	1	5	30
6	1987	1	7	26
6	1991	1	7	20
7	1990	3	10	3
9	1993	11	8	14
11	1997	11	10	14
12	1987	1	3	30
12	1987	1	4	26

Table A1. Details of Compound events (exceeding 99th percentile in both SSI and FSI) in the UKCP historical simulations (1981-2000)

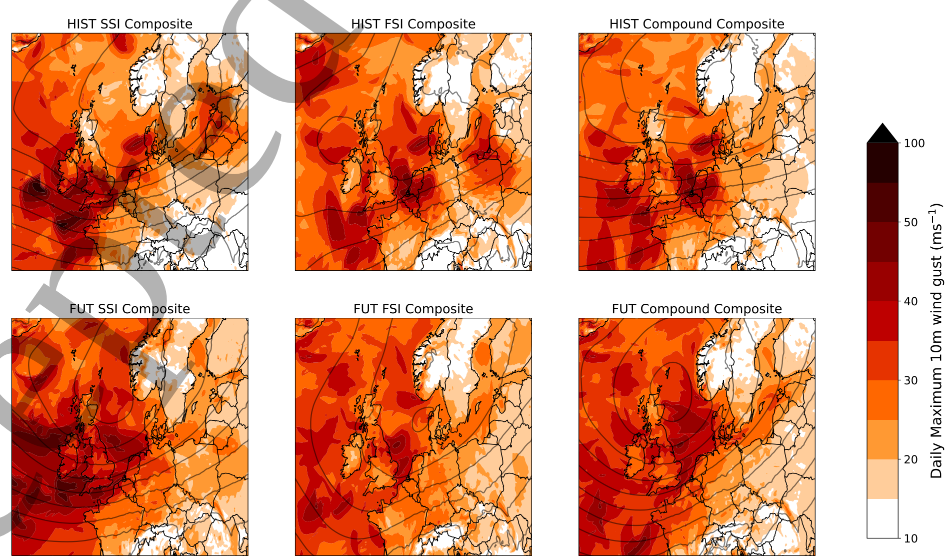

Figure A4. Daily-maximum wind gusts composites for the largest (99th Percentile) events for SSI (left) FSI (middle) and Compound events (right). Top: Historical UKCP18 period, 1981–2000, . Bottom: Future UKCP18 period, 2061–2080. Contours show MSLP composites.

Ensemble Member	Year	Month	Day	Weather Pattern
1	2063	1	19	30
1	2063	1	20	30
1	2070	1	20	30
2	2067	2	10	30
2	2069	12	10	24
2	2069	12	11	24
2	2071	1	27	26
2	2076	12	29	26
3	2072	2	21	24
3	2073	1	23	30
4	2063	2	12	24
4	2066	1	23	11
4	2069	10	27	14
5	2069	2	8	29
5	2069	2	9	30
5	2070	2	25	30
5	2074	12	2	30
5	2075	12	20	26
6	2065	2	30	29
7	2064	1	3	26
7	2073	2	10	8
7	2074	2	24	24
7	2075	1	5	30
7	2079	2	2	23
8	2068	2	8	30
8	2076	10	29	24
9	2066	1	17	30
10	2066	1	23	30
10	2067	2	12	30
10	2078	12	19	26
10	2079	1	2	30

Table A2. Details of Compound events (exceeding 99th percentile in both SSI and FSI) ensemble members 1–10. in the UKCP future simulations (2061-2080)

Ensemble Member	Year	Month	Day	Weather Pattern
11	2071	12	11	1
11	2064	2	25	30
11	2065	2	4	30
11	2068	1	9	26
11	2068	11	26	29
11	2068	11	27	24
11	2069	1	21	26
11	2071	3	2	8
11	2061	11	11	24
11	2061	11	12	14
11	2061	12	26	29
12	2063	2	3	30
12	2063	2	4	30
12	2069	2	9	30
12	2069	2	10	26
12	2071	3	11	28
12	2072	2	1	30
12	2072	2	2	30
12	2072	2	3	30
12	2075	1	16	30
12	2078	2	11	30
12	2079	2	13	30
12	2079	2	14	30
12	2079	2	16	30

Table A3. Details of Compound events (exceeding 99th percentile in both SSI and FSI) in the UKCP future simulations (2061-2080) ensemble members 11 and 12

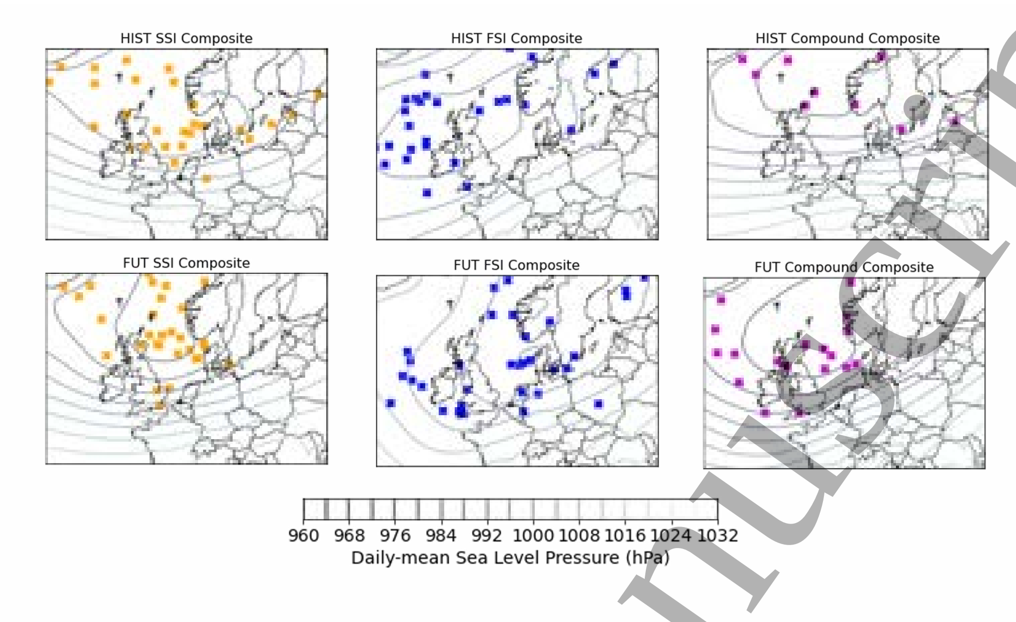

Figure A5. Mean Sea Level Pressure (MSLP) composites for the largest (¿P99) events for SSI (left) FSI (middle) and Compound events (right). Top: Historical UKCP18 period, 1981-2000, Bottom: Future UKCP18 period 2061-2080. Crosses show the minimum of MSLP during the event (note some are outside of the plot window so number of X's may not match) the number of events shown in Tables A1 to Table A3

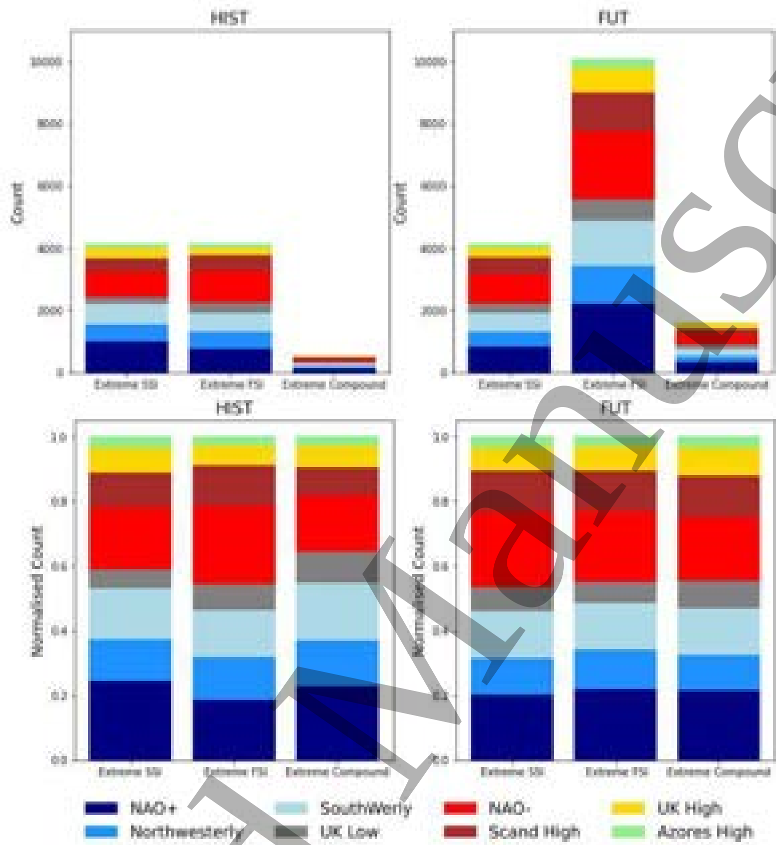

Figure A6. Top: Daily pattern occurrences during the extreme quadrants of Figure 5 (points represented by red dots). Bottom: As top, but normalised by the total number of days present in the extreme seasons.

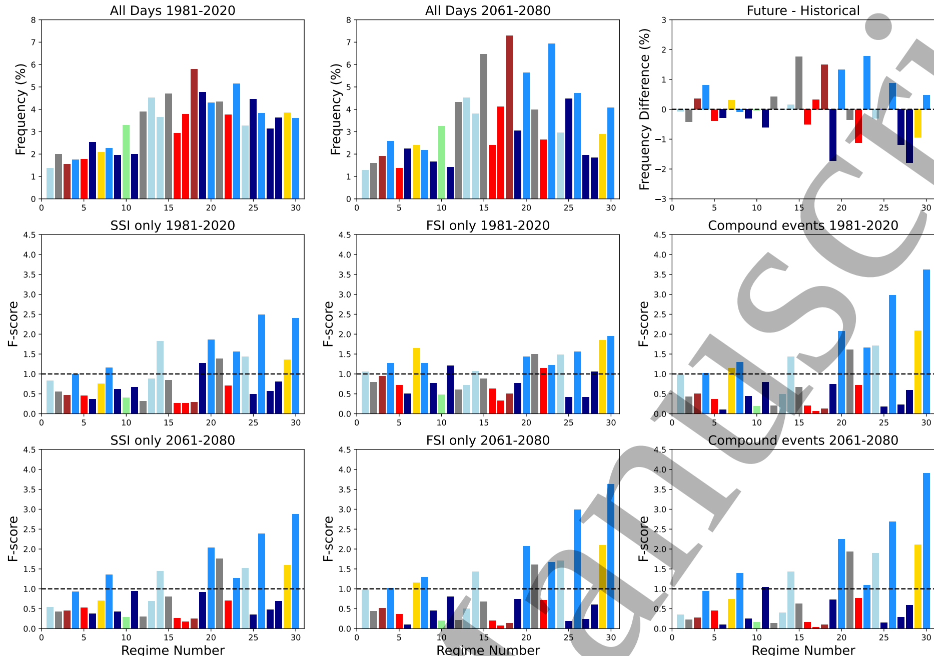

Figure A7. Impact of climate change on weather pattern characteristics. Colour classifications are taken from [39]. Top: Frequency of occurrence of the 30 weather patterns in a present and future climate. Middle: F-scores for the historical period (this is the ratio between climatological pattern occurrence, top row and conditional occurrences, see [6]). Bottom: F-scores for the future period.